INSTITUTE OF PHYSICS PUBLISHING JOURNAL OF PHYSICS: CONDENSED MATTER

J. Phys.: Condens. Matter **18** (2006) 10481–10508 doi:10.1088/0953-8984/18/46/015

Applicability of isothermal unrealistic two-parameter equations of state for solids

Papiya Bose Roy[1] **and Sushil Bose Roy**

Department of Chemistry, TM Bhagalpur University, Bhagalpur-812007, India

E-mail: papiya_boseroy@rediffmail.com

Received 25 June 2006, in final form 6 September 2006
Published 3 November 2006
Online at stacks.iop.org/JPhysCM/18/10481

Abstract

The aim of the present study, an extension of a recent one (Bose Roy and Bose Roy 2005 *J. Phys.: Condens. Matter* **17** 6193), is to assess and compare the curve-fitting utility of the isothermal unrealistic two-parameter equations of state for solids (EOS), proposed at different stages in the development of the EOS field, for the purposes of smoothing and interpolation of pressure–volume data, and extraction of accurate values of the isothermal bulk modulus and its pressure derivative. To this end, 21 such EOSs are considered, formulated by/labelled as Born–Mie (1920), Born–Mayer (1932), Bardeen (1938), Slater–Morse (1939), Birch–Murnaghan (1947), Pack–Evans–James (1948), Lagrangian (1951), Davydov (1956), Davis and Gordon (1967), Onat and Vaisnys (1967), Grover–Getting–Kennedy (1973), Brennan–Stacey (1979), Walzer–Ullmann–Pan'kov (1979), Rydberg (1981), Dodson (1987), Holzapfel (1991), Parsafar–Mason (1994), Shanker–Kushwah–Kumar (1997), Poirier–Tarantola (1998), Deng–Yan (2002) and Kun–Loa–Syassen (2003). Furthermore, all these EOSs are compared with our three-parameter EOS, as well as its two-parameter counterpart proposed in this work. We have applied all the EOS models, with no constraint on the parameters, to the accurate and model-independent isotherms of nine solids. The applicability has been assessed in terms of an unbiased composite test, comprising fitting accuracy, agreement of the fit parameters with experiment, stability of the fit parameters with variation in the compression/pressure ranges and on the basis of the number of wiggles of the data deviation curves about the fit parameters. Furthermore, a rigorous method is devised to scale the relative adequacy of the EOSs with respect to the test parameters. A number of remarkable findings emerge from the present study. Surprisingly, both the old EOSs, the Born–Mie and the Pack–Evans–James, are significantly better in their curve-fitting capability than the Birch–Murnaghan EOS which has been widely used and continues to be used for curve-fitting purposes as a standard EOS in the literature. The Born–Mayer as well as the Walzer–Ullmann–Pan'kov models also fit isotherms better than

[1] Author to whom any correspondence should be addressed.

the Birch. The performance of the EOS based on the Rydberg potential—that has been rediscovered by Rose *et al* (1984 *Phys. Rev.* B **29** 2963), and strongly promoted by Vinet *et al* (1989 *J. Phys.: Condens. Matter* **1** 1941) as the so-called universal equation of state, and is currently used as a standard EOS along with that of the Birch—is very poor, on a comparative scale. Furthermore, the curve-fitting capability of our original three-parameter EOS, and more importantly its two-parameter counterpart, is superior to all the isothermal unrealistic two-parameter EOSs so far proposed in the literature.

(Some figures in this article are in colour only in the electronic version)

1. Introduction

A fundamental problem in high-pressure research is the formulation of a well-behaved equation of state (EOS) for solids which should be capable of accurately representing the curvature of the experimental compression data ranging to high pressures. A successful EOS model based on a complete physical basis would provide an insight into the esoteric nature of the variation of the interatomic interaction that comes into play with the increasing pressure. But unfortunately no such model is known to date. Derivation of the exact equation of state for solids is a many-body interaction problem. Because of the highly complex nature of the variation of the interatomic interaction with increasing pressure, a theoretical idealization of the exact physical situation entailing the changes in the widely varying structural and bonding characteristics of solids has thus far proved elusive. However, the question as to which of the several existing empirical EOS models is likely to be most appropriate, that is which one is the closest approximation to the experimental situation, is of considerable importance in the largely empirical EOS field, and needs to be addressed.

Theoretical efforts to derive equation of state for solids, using various techniques [1–5], have thus far failed to provide a viable alternative for the role of an empirical EOS model, and consequently on the completion of a time-consuming expensive experiment on the compression of solids one continues to look for an EOS that behaves best for the purposes of smoothing and interpolating pressure–volume data, and extracting accurate values of thermodynamic parameters like the isothermal bulk modulus and its pressure derivative. An EOS model finds numerous important applications [6–10], and is important in its own right. EOSs now have to face new challenges in view of the advances on the experimental front [11, 12], especially the horrendous pressure and temperature ranges now achievable in the laboratory environment [13], in order to prove their adequacy.

Various empirical functional forms, based on different implicit and explicit assumptions, have been proposed in the literature, for over a century now; proponents of all of them claiming an accurate representation of the experimental pressure–volume data. A survey of the high-pressure literature clearly reveals that most of the EOSs have not been compared with all the existing EOSs to assess their curve-fitting capability for the laboratory compression data. And in most cases where a comparison is made it is restricted to a few of the existing EOSs, best suited to the authors, to uphold the superiority or utility of their proposed models—and that too often in line with an inappropriate and inadequate method and not infrequently using model-biased data. This is why a widespread misunderstanding has arisen in the literature regarding the relative curve-fitting capability of the existing EOSs. In a recent study [14] we established an unbiased stringent discrimination technique for establishing a ‘preferred’ representation for

the curve of a set of compression data; and compared a number of isothermal three-parameter EOSs, considered viable at different stages in the development of the EOS field. Applying this discrimination technique we arrived at a secure conclusion on the curve-fitting capability of three-parameter EOSs, and showed that our three-parameter EOS [15] is superior to all the three-parameter EOSs thus far proposed in the literature. The aim of the present study is to extend the work to the intercomparison of the curve-fitting capability of the two-parameter EOSs, following a discrimination technique—the harshest ever designed and applied in the literature—and thus to put to rest any speculation with regard to their curve-fitting capability. There is a plethora of rival isothermal two-parameter EOSs in the literature, and it would be an unwieldy exercise to compare the curve-fitting capability of all of them in a single paper; and this is why we have confined ourselves in the present work to the unrealistic EOSs, i.e. to those expressible in the $P = f(V/V_0)$ forms, only. We have compared our original three-parameter EOS along with its two-parameter counterpart with 21 one such existing unrealistic EOSs in the literature.

2. Empirical equations of state

The science of high-pressure equations of state for solids is a largely empirical field. In this section we present as many as 21 empirical isothermal two-parameter EOSs, expressible in unrealistic forms only—along with our three-parameter realistic EOS and its realistic two-parameter counterpart. Constancy of temperature is assumed throughout and no special notation is used. V and V_0 denote volume at pressure P and zero, respectively, and $x = (V/V_0)^{1/3}$ is the linear compression. While B_0, B_0' and B_0'' denote the isothermal bulk modulus and its first and second pressure derivatives, respectively, at zero pressure.

A potential function of the general form based on the century-old potential (1903) proposed by Mie [17] and extended by Gruneisen [18, 19], is

$$E(r) = -A(a/r)^m + B(a/r)^n. \tag{1}$$

Here a is the equilibrium (zero-pressure) value of atomic spacing r. A and B are positive constants with the dimensions of energy and m, n are dimensionless indices ($n > m$), often, but not necessarily, integers. Commonly the first term is identified as an attractive term and the second as a repulsive one, but this is not a necessary interpretation [20].

The three-parameter EOS built on this well-known potential [21], which is the precursor of a number of EOSs and hereafter referred to as Mie–Gruneisen EOS, is

$$P = \{3B_0/(n-m)\}[(V/V_0)^{-\{1+(n/3)\}} - (V/V_0)^{-\{1+(m/3)\}}], \tag{2}$$

where, $n = 3[(1/2)(B_0'^2 + 4B_0B_0'')^{1/2} + (1/2)B_0' - 1]$, $m = 3[(1/2)B_0' - 1 - (1/2)(B_0'^2 + 4B_0B_0'')^{1/2}]$, and $(n-m) = 3(B_0'^2 + 4B_0B_0'')^{1/2}$.

It may be noted here that a number of EOSs have appeared in the literature where m and n are regarded as disposable parameters with specific choices. Born [22] suggested that $m = 1$ be favoured as a representation of electrostatic attraction, and thus equation (1), retaining the inverse power form for the short-range repulsive potential energy, leads to the well-known two-parameter Born–Mie EOS [23–26]. It will be interesting to note that over five decades ago Ramsey dealt at length with the limits and applicability of the following Born–Mie EOS ([24], and citations therein), in the context of geophysical data:

$$P = [3B_0/(3B_0' - 8)] \times [(V/V_0)^{\{(4/3)-B_0'\}} - (V/V_0)^{-4/3}] \tag{3}$$

Walzer, Ullmann and Pan'kov (1979) [27] as well as Ullmann and Pank'ov [28] suggested the use of the Mie–Gruneisen EOS (1), but with a requirement that $n = 2m$, so that

$m = (B_0' - 1)$ and $n = 2(B_0' - 1)$. And thus they favoured the pressure–volume relation

$$P = \{3B_0/(B_0' - 2)\}[\{(V/V_0)^{-[1+\{(2(B_0'-2))/3\}]}\} - \{(V/V_0)^{-[1+\{\{B_0'-2)/3\}]}\}]. \quad (4)$$

While in the Born–Mayer potential [29–31],

$$\phi = -Aa/r + B\exp(-fa/r), \quad (5)$$

the power-law repulsion of the Mie potential is replaced with an exponential repulsion, in line with the teachings of quantum mechanics; but the electrostatic attractive term, of the Madelung-type $1/r$ as suggested by Born, is retained. f is related to B_0':

$$f = (3/2)(B_0' - 1) + (3/2)[B_0'^2 - (14/3)B_0' + (19/3)]^{1/2}, \quad (6)$$

and the EOS obtained is

$$P = \{3B_0/(f - 2)\}[((V/V_0)^{-2/3})\{\exp f(1 - (V/V_0)^{1/3})\} - (V/V_0)^{-4/3}]. \quad (7)$$

An EOS that has been widely used for over five decades now, as a standard EOS in the literature, is the Birch–Murnaghan EOS [32–37]. It is founded on a stress–strain formalism based on the bulk property of an elastic solid. As is well known in continuum mechanics that there is no unique frame of reference that describes finite deformations, and as such there is no unique definition of strain [37–39]. This ambiguity necessitated the use of a 'generalized' definition of the strain variable for quantifying volumetric compression [40, 41],

$$f = (1/n)[(V_0/V)^{n/3} - 1]. \quad (8)$$

Defined this way, the strain is positive on compression, and it is assumed to be isotropic [42]. Here n is just a parameter that allows one to vary the strain from an Eulerian ($n = 2$) to a Lagrangian ($n = -2$) frame of [43].

Birch [34] expanded the free energy as a Taylor power series in Eulerian strain measure and obtained the following two-parameter EOS, on truncation at the third-order term of energy in strain:

$$P = 3B_0 f(1 + 2f)^{5/2}[1 + a_1 f + \cdots] \quad (9)$$

with $a_1 = 3/2(B_0' - 4)$, and $f = (1/2)[(V/V_0)^{-2/3} - 1]$.

This equation has achieved prominence in the literature as the Birch–Murnaghan EOS through its application by Birch [32–36] and others to problems of finite compression in the interior of the earth. It was apparently first written by Murnaghan [43] in an early exposition of the thoughts which led eventually to his 1951 treatise [44].

A similar exercise of expansion of the free energy as a Taylor power series in Lagrangian strain measure, and truncation, yields the third-order Lagrangian isotherm:

$$P = (3/2)B_0[(V/V_0)^{-1/3} - (V/V_0)^{1/3}][1 - (3/4)B_0'\{(V/V_0)^{2/3} - 1\}]. \quad (10)$$

This equation appears in Murnaghan's 1951 monograph [37, 44]. It is important to note here that approximations made in free energy, required for application to real solids, affect the results of the choice of a definition of strain, and hence the stress–strain relations, equations (9) and (10), are not exact.

Further, it will be interesting to note that the Mie–Gruneisen equation (1), with $m = 2$ and $n = 4$, yields the same two-parameter Birch–Murnaghan EOS as given in equation (9).

An EOS was derived by Bardeen from quantum mechanics [20, 40, 45] using the Wigner–Seitz model [46, 47] to explain compressions of alkali metals:

$$P = 3B_0[(V/V_0)^{-5/3} - (V/V_0)^{-4/3}][1 + (3/2)(B_0' - 3)\{(V/V_0)^{-1/3} - 1\}]. \quad (11)$$

Considerations by Gombas [48] suggested the possibility of a wider application in the case of metals. However, we are interested in investigating the generality of its application. Furthermore, it will be interesting to note that the Bardeen EOS is equivalent to the two-parameter equation of state obtained with $n = 1$ in the generalized strain (8).

The first quantum-based potential, that continues to assume importance in the theoretical thermodynamic studies of solids, was proposed by Morse [49, 50] to explain the vibrational spectrum of the H_2 molecule, and is presented as

$$\phi = A\{\exp[2f(1-(r/a))] - 2\exp[f(1-(r/a))]\}. \tag{12}$$

where the constant A is the binding energy at equilibrium spacing a, and $r/a = (V/V_0)^{1/3}$. Slater [51] used this potential in a finite strain theory to generate an EOS for solids:

$$P = (x^{-2})\{3B_0/(B_0'-1)\}[\exp(2(B_0'-1)(1-x)) - \exp((B_0'-1)(1-x))], \tag{13}$$

with $f = (B_0' - 1)$.

Shortly afterwards Rydberg [52] came up with a modified version of the Morse potential, achieving an improved fit to the vibrational spectrum of diatomic molecules,

$$\phi = A[1 - f(1-(r/a))][\exp\{f(1-(r/a))\}]. \tag{14}$$

This potential leads to an EOS,

$$P = 3B_0(1-x)(x^{-2})\exp[(3/2)(B_0'-1)(1-x)]. \tag{15}$$

Equation (15), based on the Rydberg atomic potential function, appears in a catalogue of finite strain theories that were compared with seismological data (equation (102) in [20]). Rose *et al* rediscovered it [53] and Vinet *et al* [54, 55] dubbed it a universal equation of state. Currently it has been referred to as the 'Vinet equation', obviously a misnomer. Perhaps, typographical errors in the aforesaid equation (102) [56] or apparently an ignorance of its long history [21] might have hindered an immediate appreciation of the resemblance between the two.

Equation (15) is based on certain empirical observations of universal scaling behaviour in the binding energies of metal as reported by Rose *et al* [53, 57–59]. It is based on an expression for the cohesive energy of a condensed system that is assumed to vary only as a function of a normalized interparticle separation (a^*). Specifically, the energy is given in normalized form as $E^*(a^*) = -(1 + a^* + \cdots)\exp(-a^*)$, in which higher-order terms in the Taylor expansion are ignored in deriving equation (15). The presence of the exponential term in the energy has been explained in a general way as reflecting the typical form of interatomic repulsions [60]. However, although the work of Rose *et al* [57] is based on metallic adhesive binding-energy calculations, the universal scaling behaviour reported by them is not the result of any underlying theory of structural energetics, and is thus empirical in nature [61].

Davydov [20, 62, 63] proposed a potential, akin to both the Morse and Rydberg expressions, as

$$E(r) = \{A(a/r) - B\}[\exp\{f(1-(a/r))\}], \tag{16}$$

and the EOS resulting from the above potential is

$$P = \{3B_0/(f+2)\}[x^{-4} + fx^{-3} - (f+1)x^{-2}][\exp\{f(1-x)\}]. \tag{17}$$

Here, $f = (3/4)[(B_0' - 3) + \{(B_0' + 1)(B_0' - (5/3))\}^{1/2}]$.

Pack *et al* [64] recognized that quantum-mechanical theories indicated that the repulsive components in atomic potentials depend exponentially upon atomic separation. They further argued that at very high pressures the attractive components become insignificant and they therefore proposed a finite strain relationship that neglected them [20]:

$$P = \{B_0/(B_0'-1)\}\{\exp[3(B_0'-1)\{1-(V/V_0)^{1/3}\}] - 1\}\{(V/V_0)^{-2/3}\}. \tag{18}$$

Davis and Gordon [65] formulated a two-parameter analytical equation for the pressure dependence of the volume, using a Taylor series expansion of the pressure in powers of V_0/V, about $V_0/V = 1$ or $V = V_0$, and restricting to the quadratic term,

$$P = B_0\{(x^{-3}) - 1\} + (1/2)B_0(B_0' - 1)\{(x^{-3}) - 1\}^2. \tag{19}$$

Following an alternative though related approach, Onat and Vaisnys [65] expanded the pressure in powers of $\ln V$ about $V = V_0$, and formulated the following expression:

$$P = -B_0(\ln x^3) + (1/2)B_0B_0'(\ln x^3)^2 \tag{20}$$

Grover *et al* (1973) [66, 67] observed that isothermal compression data derived from shock-wave and static compression measurements on metals exhibit a nearly precise linear relation between the logarithm of the bulk modulus and the specific volume up to volume changes of 40%. This observation prompted them to represent the increase in B with P as a logarithmic dependence on volume compression, $\Delta V/V_0 = (V_0 - V)/V_0 = (1 - V/V_0)$,

$$\ln B = \ln B_0 + \alpha\{1 - (V/V_0)\}. \tag{21}$$

However, the series solution of the $P(V/V_0)$ relationship in the form of an exponential integral, obtainable on integration of equation (21), is not sufficiently convergent to be useful [20], implying that this equation cannot be integrated to obtain $P(V/V_0)$ in terms of simple functions. Recognizing this inconvenient position, Grover *et al* presented an expression, in line with the suggestion of Vaidya [66],

$$B = B_0 + \{(\alpha + (V_0/V))/(\alpha + 1)\}[\exp\{\alpha(\Delta V/V_0)\}]. \tag{22}$$

On differentiating equation (22) with pressure, and putting $V = V_0$ at $P = 0$, two values of α in terms of B_0' are obtained, of which the negative value of α, being physically implausible, is discounted. And thus the EOS formulated by Grover *et al* is

$$P = \{B_0/(\alpha + 1)\}[\{(V_0/V)(\exp\alpha(1 - (V/V_0)))\} - 1], \tag{23}$$

with, $\alpha = [(B_0' - 1) + (B_0'^2 + 2B_0' - 3)^{1/2}]/2$.

It is important to note that the original equation (21) for the bulk modulus yields the following relationship:

$$B' = B_0'(V/V_0). \tag{24}$$

In the limit $P \to \alpha$, $V/V_0 \to 0$ and equation (24) leads to $B' \to 0$. While equation (22), under similar situations, predicts $B' \to 1$. Thus equation (22), unlike equation (21), is not in conflict with the thermodynamic dictum $B_\alpha' \geqslant 1$ [68], and as such is more consistent with the theoretical point of view. Further, it may be noted that equation (23) used by us in the present study is different from the other forms of EOS attributed to Grover *et al* [69–71].

With the classical assumption of the constancy of C_v, at sufficiently high temperatures (and in minerals that are not too near to phase transitions), one can have the thermal Gruneisen parameter γ inversely proportional to density ρ. Coupling this equation with the free volume formulation for γ [72] and taking the second Gruneisen constant $q = 1$, Brennan and Stacey [73] proposed the following high-pressure EOS, apparently based on a clear thermodynamic basis:

$$P = \{3B_0/(3B_0' - 5)\}\{(V/V_0)^{-4/3}\}[\{\exp((3B_0' - 5)/3)(1 - (V/V_0))\} - 1]. \tag{25}$$

The first well-founded theoretical indication that there was some degree of universality in the compressibility of metals came from the extensive density-functional calculations of the ground states of elemental solids performed by Moruzzi and co-workers [74]. Taking a cue

from their observation of a universal relation between the bulk modulus and interstitial electron density, Dodson [61] has suggested an empirical EOS:

$$P = \{1.5B_0/(1-\beta)^2\}[(1/x^2) - (4\beta/x) - 2\beta^2(\ln x) + 4\beta - 1], \tag{26}$$

where $\beta = 1 - (2/3B_0')$.

Following an idea [75, 40] vigorously pursued, Holzapfel [76, 77] argued that at extreme pressure all materials are expected to convert to a Thomas–Fermi state [78, 79], and that equations of state should extrapolate smoothly to meet the Thomas–Fermi theory, which requires $B_\infty' = 5/3$. And accordingly the Rydberg EOS (15) was tailored, imparting to it the desired asymptotic attribute to suit the Thomas–Fermi condition at very strong compression, and thus generating a modified version of the Rydberg EOS:

$$P = 3B_0(V/V_0)^{-5/3}\{1 - (V/V_0)^{1/3}\}\exp[C_{02}\{1 - (V/V_0)^{1/3}\}], \tag{27}$$

with $C_{02} = (3/2)(B_0' - 3)$.

Stacey *et al* [21, 80], however, pointed out that equation of state parameters cannot survive the phase transitions that inevitably intervene on the pathway to the extreme Thomas–Fermi condition. They further argued that parameters for the Thomas–Fermi state have no relevance to normal materials, and B_∞' for a material in its observed state is not related to properties of something that it does not in the least resemble—and thus equation (27) lacks a theoretical justification.

Parsafar and Mason [81] derived a universal equation of state for compressed solids, based on thermodynamic arguments applied to virial expansions of $E(\rho, T)$ and $\rho(\rho, T)$, of the form $\rho(V/V_0) = A_0 + A_1(\rho/\rho_0) + A_2(\rho/\rho_0)^2$ as

$$P = \{(1/2)B_0(x^{-6})\}[(B_0' - 7) - 2(B_0' - 6)(x^{-3}) + (B_0' - 5)(x^{-6})]. \tag{28}$$

Shanker *et al* [82] formulated an equation of state using a combined form of an inverse power dependence and exponential dependence for the short-range force constant on volume, as

$$P = [\{B_0(x^{-4})\}/t][\{1 - (1/t) + (2/t^2)\}\{\exp(ty) - 1\} + y\{1 + y - (2/t)\}\exp(ty)], \tag{29}$$

where $y = 1 - x^3$ and $t = B_0' - 8/3$.

Based on the Hencky logarithmic strain, Poirier and Tarantola [83] arrived at an EOS,

$$P = [B_0(x^{-3})][(\ln(x^{-3})) + ((B_0' - 2)/2)(\ln(x^{-3}))^2]. \tag{30}$$

They claimed that their Hencky measure of strain is superior to that of the Eulerian strain used by Birch. Gaurav *et al* [56], using a typical value for B_0', demonstrated that the free energy expansion to fourth order in powers of Hencky strain is not convergent, contrary to their claim, unlike that of Eulerian strain. It will be interesting to study their claim in the light of their capability to describe the model-independent data.

The phenomenological EOS derived by Deng and Yan [84], within the framework of the theory of lattice potential for ionic crystals, and based on the Born–Mayer exponential potential model [31] and the method developed by Shanker *et al* (1997) [82], is

$$P = \{3B_0/(3B_0' - 8)\}\{(V/V_0)^{-4/3}\}[((V/V_0)^{2/3})\{\exp\{3(B_0' - 2)(1 - (V/V_0)^{1/3})\}\} - 1]. \tag{31}$$

Kunc *et al* (2003) [85] calculated the pressure–volume relationship of cubic diamond, an archetype of the covalently bonded tetrahedrally coordinated insulators, based on density-functional theory within the local-density approximation and the generalized gradient approximation. They needed to identify an analytical form of the $P(V)$ behaviour which, using their theoretically calculated stress-free bulk moduli parameters, fits the calculated pressures

over the full volume range. They tried several of the existing EOSs and finally identified the best analytical expression, in the least-squares sense, as

$$P = \{3B_0(V/V_0)^{-n/3}\}\{1-(V/V_0)^{1/3}\}[\exp\{\eta(1-(V/V_0)^{1/3})\}], \tag{32}$$

where $\eta = (3B_0'/2) + (1/2) - n$ and $n = 7/2$. With $n = 7/2$, equation (32) is a blend of the Rydberg form and the Holzapfel expression, for which $n = 2$ and $n = 5$, respectively.

Bose Roy and Bose Roy [14–16] proposed an isothermal empirical EOS model,

$$V/V_0 = 1 - [(\ln(1+aP))/(b+cP)]. \tag{33}$$

Putting $m = [3(B_0'+1)\{(25B_0'^2 + 18B_0' - 32B_0B_0'' - 7)^{1/2}\}]$, one obtains

$$a = (m/8B_0), \qquad b = (m/8), \qquad \text{and} \qquad c = [(m/16)\{(B_0'+1) - (m/8)\}].$$

In order to assess the robustness of this three-parameter model, it is reduced to a two-parameter EOS by imposing a constraint $(B_0'/B_0) = -B_0''$ on equation (33). Putting $n = [3(B_0'+1)\{(25B_0'^2 + 50B_0' - 7)^{1/2}\}]$, the pressure-independent parameters for the new two-parameter EOS (equation (34)), reduces to

$$a = (n/8B_0), \qquad b = (n/8); \qquad \text{and} \qquad c = [(n/16)\{(B_0'+1) - (n/8)\}].$$

We label the original three-parameter EOS (33) as Bose Roy–Bose Roy* to distinguish it from the two-parameter EOS (34), labelled as Bose Roy–Bose Roy, throughout the study.

3. Application to model-independent isotherms

All the 23 EOSs presented in section 2 are fitted to the EOS data of nine solids, namely Ag, Al, Cu, Mg, Pd, MgO [86], NaCl [87] and Mo and W [88]—corresponding to the regression curves of P on V/V_0. A departure from our previous study [14], with respect to the use of the isotherm of Cu, may be noted here. In the present study, the model-independent isotherm of Cu ranging to 1600 kbar is chosen instead of Nellis *et al*'s isotherm of Cu [89] ranging to the terapascal regime. We have noted that none of the 22 isothermal two-parameter EOSs considered succeed in successfully describing the curvature of the ultra-high-pressure isotherm of Cu [89]. An obvious limitation of the two-parameter EOSs in describing the ultra-high-pressure/compression of isotherms is thus immediately apparent. The EOS data considered are model-independent and accurate enough to allow a meaningful discrimination between the curve-fitting capabilities of the EOSs, as noted in our recent study [14]. The original isotherms of the above solids, referred to hereafter as the high-pressure isotherms, are abbreviated as HPIs. The subsets of these HPIs, from the pressure values $P = 0$ to a low-pressure maximum, referred to hereafter as low-pressure isotherms, are abbreviated as LPIs. Table 1 shows the details related to these HPIs and LPIs. The experimental bulk modulus values, chosen for the purpose of comparison with the fit parameters for HPIs, are presented in table 2. The rationale for selecting these bulk moduli data has been discussed in our earlier work [16]. The root-mean-square deviations (RMSDs) between the data points (HPIs) and fits are reported in table 3. The values of the bulk modulus parameters, as such, are not shown. The deviation parameters, D_i $(i = 1, 2, 3, 4)$, which are more important and meaningful for comparing the applicability of the EOSs, are computed instead, and summarized in tables 4–7. D_1 values refer to the percentage deviations of the fit values of B_0 inferred from the HPIs from those of the fit values of B_0 inferred from the LPIs, for all the isotherms of the solids considered. Likewise, D_2 values refer to the corresponding deviations of B_0'. While D_3 and D_4 values are the percentage deviations of the fit parameters B_0 and B_0' from the corresponding experimental values. It may be noted that since our three- and two-parameter EOSs cannot be explicitly expressed in the unrealistic form, we have implicitly calculated the regression curves of P on V/V_0 for them

Table 1. Details related to the isotherms of solids and their subsets, used in the study. n denotes the number of data points.

			High-pressure isotherm (LHPI)			Low-pressure isotherm (HLPI)		
Solids	Reference	T (K)	n	P_{max} (kbar)	MRV[a]	n	P_{max} (kbar)	MRV[a]
Ag	[86]	293	57	1500	0.6519	29	145	0.9017
Al	[86]	293	49	1100	06083	20	100	0.9010
Cu	[86]	293	59	1600	0.6624	30	150	0.9150
Mg	[86]	293	41	700	0.5510	8	40	0.9081
Mo	[88]	293	30	3000	0.6305	8	800	0.8167
Pd	[86]	293	67	2000	0.6831	32	250	0.9018
W	[88]	293	30	3000	0.6552	8	800	0.8347
MgO	[86]	293	51	1200	0.7046	31	200	0.9017
NaCl	[87]	293	40	200	0.7023	8	40	0.8849

[a] Minimum relative volume.

Table 2. Experimental values of B_0 and B_0' used for comparison purposes.

Solids	B_0 (Expt.) (kbar)	Reference	B_0' (Expt)	Reference
Ag	1047[a]	[90]; [91]	5.53	[92]
Al	742 ± 8	[93]	4.72	[94]
Cu	1374[b]	[90]; [91]; [97]	5.25	[95]
Mg	344.20	[96]	4.16	[96]
Mo	2653	[90]	4.5 ± 0.5	[97]
Pd	1808	[91]	5.3 ± 0.2	[97]
W	3084	[98]	4.0 ± 0.2	[97]
MgO	1560	[99]	4.52	[100]
NaCl	238.35	[101]	5.11	[102]

[a] An average of two values.
[b] An average of three values.

and compared the results with those from the explicit curve-fittings of P on V/V_0 for the rest of the EOSs, for the sake of definitiveness in comparison.

3.1. Fitting accuracy; fit parameters—stability and agreement with experiment

In our previous study [14] we adopted a simple statistical path, wherein an EOS for which deviation points for five or more isotherms (against a total of nine isotherms considered) were lower in magnitude, compared to those of others, was credited with a higher adequacy on a relative scale of adequacy. In the present study, however, we have devised a rigorous but simple method, comprising two complementary approaches to assess the relative adequacy of the EOSs with respect to the test parameters entailing the deviation points, i.e. D_1, D_2, D_3, D_4 and RMSD. In the first approach, labelled the collective isotherm approach (CIA), the inconsistency (non-uniformity) between the deviation points is taken into consideration. The deviation points (DPs), inferred from an EOS for all the nine isotherms, are arranged in a row in ascending order

Table 3. Root-mean-square deviations (RMSDs) (in kbar) between the data points and fits corresponding to the regression curves of P on V/V_0 (in kbar) for selected solids.

	2-parameter EOSs	Ag	Al	Cu	Mg	Mo	Pd	W	MgO	NaCl
1	Bose Roy–Bose Roy*	0.18	0.20	0.19	0.19	1.03	0.24	0.36	0.23	0.08
2	Bose Roy–Bose Roy	0.89	0.55	0.79	0.46	1.04	1.13	0.40	0.54	0.48
3	Born–Mie	1.73	0.45	1.21	0.86	1.39	1.46	0.69	0.45	0.50
4	Pack–Evans–James	2.04	0.52	1.41	1.07	1.59	1.70	0.77	0.49	0.49
5	Walzer–Ullmann–Pan'kov	2.65	0.53	1.89	1.06	1.58	2.40	0.75	0.71	0.46
6	Born–Mayer	2.85	0.94	2.19	1.49	2.58	2.58	1.60	0.94	0.42
7	Birch–Murnaghan	3.19	0.47	1.93	0.98	1.78	2.85	0.86	0.61	0.47
8	Deng–Yan	2.85	0.94	2.19	1.49	2.58	2.58	1.60	0.94	0.42
9	Parsafar–Mason	2.28	1.51	1.74	2.05	5.82	2.04	4.34	0.96	0.41
10	Holzapfel	3.83	0.96	2.86	1.46	2.23	3.60	1.32	1.14	0.38
11	Grover–Getting–Kennedy	4.06	1.72	3.14	2.29	4.08	3.64	2.81	1.26	0.35
12	Kunc–Loa–Syassen	4.17	1.31	3.21	1.76	3.03	3.97	2.06	1.36	0.35
13	Slater–Morse	4.10	1.47	3.23	1.89	3.51	3.91	2.48	1.42	0.34
14	Davydov	4.23	1.35	3.27	1.79	3.11	4.03	2.13	1.39	0.34
15	Bardeen	6.00	0.91	4.00	1.39	1.79	5.67	0.94	1.32	0.36
16	Shanker–Kushwah–Kumar	4.76	2.05	3.83	2.44	4.67	4.49	3.45	1.68	0.29
17	Rydberg	3.99	1.67	3.57	2.05	3.89	4.33	2.83	1.58	0.31
18	Brennan–Stacey	4.99	2.23	4.06	2.54	5.09	4.76	3.87	1.86	0.26
19	Dodson	9.37	3.77	7.31	3.72	7.55	9.10	6.05	3.08	0.10
20	Davis–Gordon	9.90	2.50	7.19	2.56	4.04	9.72	3.11	2.70	0.16
21	Poirier–Tarantola	10.9	3.43	8.15	3.31	6.19	10.7	4.99	3.23	0.11
22	Onat–Vaisnys	22.4	11.4	18.8	9.29	23.7	23.1	20.3	8.53	0.90
23	Lagrangian	26.9	14.7	23.0	11.7	31.4	28.0	27.1	10.7	1.28

Table 4. Percentage deviations in the fit values of B_0 for the HPI from those of B_0 for the LPI, denoted by D_1 in the text.

	2-parameter EOS	Ag	Al	Cu	Mg	Mo	Pd	W	MgO	NaCl
1	Bose Roy–Bose Roy*	0.57	1.32	0.30	0.18	0.34	0.38	0.45	−0.13	−0.29
2	Bose Roy–Bose Roy	−0.95	1.53	−0.74	0.94	0.26	0.98	0.29	−0.91	4.83
3	Born–Mie	−1.23	1.28	−0.74	−0.68	0.30	−0.76	0.58	−0.52	5.33
4	Pack–Evans–James	−1.61	1.06	−0.81	−1.09	0.11	−0.93	0.45	−0.52	5.29
5	Walzer–Ullmann–Pan'kov	−3.22	0.60	−2.00	−1.50	0.00	−2.30	0.26	−1.05	4.75
6	Born–Mayer	−3.41	−0.50	−2.45	−3.06	−1.09	−2.46	−0.61	−1.44	4.21
7	Birch–Murnaghan	−4.26	0.88	−2.00	−1.23	−0.30	−3.01	0.10	−0.85	5.05
8	Deng–Yan	−3.41	−0.50	−2.45	−3.06	−1.09	−2.46	−0.61	−1.44	4.21
9	Parsafar–Mason	−2.46	−1.85	−1.78	−5.12	−3.43	−1.75	−2.52	−1.50	4.09
10	Holzapfel	−5.64	−0.67	−3.78	−3.15	−0.82	−4.21	−0.39	−1.83	3.71
11	Grover–Getting–Kennedy	−5.11	−1.75	−3.56	−5.09	−2.10	−3.60	−1.32	−1.83	3.63
12	Kunc–Loa–Syassen	−6.24	−1.53	−4.38	−4.35	−1.58	−4.82	−1.06	−2.22	3.22
13	Slater–Morse	−6.10	−1.89	−4.38	−4.86	−2.03	−4.71	−1.42	−2.35	3.09
14	Davydov	−6.38	−1.64	−4.53	−4.50	−1.69	−4.93	−1.13	−2.29	3.18
15	Bardeen	−10.2	−0.52	−5.94	−2.82	−0.34	−7.73	−0.03	−2.16	3.30
16	Shanker–Kushwah–Kumar	−6.98	−2.95	−5.12	−6.45	−2.89	−5.20	−2.10	−2.68	2.55
17	Rydberg	−6.97	−2.40	−5.05	−5.53	−2.40	−5.37	−1.71	−2.62	2.72
18	Brennan–Stacey	−7.51	−3.54	−5.72	−7.16	−3.39	−5.75	−2.55	−3.08	2.13
19	Dodson	−16.5	−7.19	−11.7	−12.4	−5.78	−12.8	−4.54	−5.31	−0.97
20	Davis–Gordon	−19.2	−4.79	−12.4	−8.66	−2.82	−14.9	−2.23	−4.85	−0.42
21	Poirier–Tarantola	−21.4	−7.05	−14.2	−12.1	−4.95	−16.6	−3.95	−5.84	−1.81
22	Onat–Vaisnys	−50.1	−29.5	−36.9	−47.9	−26.0	−39.9	−21.0	−16.7	−18.4
23	Lagrangian	−62.2	−39.7	−46.6	−65.7	−37.0	−49.8	−29.7	−21.3	−26.2

Table 5. Percentage deviations in the fit values of B_0' for the HPI from those of B_0' for the LPI, denoted by D_2 in the text.

	2-parameter EOS	Ag	Al	Cu	Mg	Mo	Pd	W	MgO	NaCl
1	Bose Roy–Bose Roy*	−2.81	−10.1	−1.28	−6.46	−1.45	−1.65	−2.63	0.58	1.87
2	Bose Roy–Bose Roy	0.52	−3.95	0.20	−2.74	−0.54	0.97	−0.69	2.63	−9.07
3	Born–Mie	0.24	−4.51	−0.62	−1.53	−0.99	0.08	−1.60	1.34	−10.3
4	Pack–Evans–James	0.54	−4.20	−0.56	−0.97	−0.63	0.13	−1.34	1.24	−10.3
5	Walzer–Ullmann–Pan'kov	4.43	−2.99	2.55	0.36	−0.31	3.65	−0.92	3.09	−9.25
6	Born–Mayer	4.45	−0.41	3.34	3.76	1.95	3.71	1.11	4.17	−7.88
7	Birch–Murnaghan	7.20	−3.55	2.75	−0.24	0.23	5.61	−0.49	2.43	−10.1
8	Deng–Yan	4.06	−0.35	3.00	3.22	1.60	3.39	0.93	3.66	−7.07
9	Parsafar–Mason	2.80	2.16	1.90	6.87	5.33	2.31	4.42	4.15	−7.29
10	Holzapfel	9.69	0.14	7.00	4.38	1.44	8.18	0.71	5.78	−7.12
11	Grover–Getting–Kennedy	6.93	1.87	5.15	7.26	3.92	5.41	2.64	4.93	−6.84
12	Kunc–Loa–Syassen	11.2	2.35	8.61	7.25	3.24	9.52	2.35	7.09	−5.89
13	Slater–Morse	10.7	3.21	8.51	8.37	4.13	9.14	3.16	7.31	−5.54
14	Davydov	11.4	2.62	8.86	7.60	3.42	9.75	2.50	7.28	−5.73
15	Bardeen	25.0	−0.07	14.5	3.90	0.34	19.8	−0.28	7.48	−6.57
16	Shanker–Kushwah–Kumar	11.6	5.41	9.73	11.7	6.01	9.80	4.70	8.21	−4.44
17	Rydberg	12.7	4.53	10.2	10.1	4.95	10.8	3.93	8.36	−4.69
18	Brennan–Stacey	12.9	7.11	11.1	13.6	7.07	11.0	5.82	9.49	−3.30
19	Dodson	40.3	18.8	30.6	30.7	13.9	32.7	11.8	18.6	4.29
20	Davis–Gordon	60.5	13.8	39.1	23.0	7.42	47.4	6.26	19.0	3.60
21	Poirier–Tarantola	68.7	21.2	45.9	34.3	13.2	53.7	11.3	23.0	7.62
22	Onat–Vaisnys	281	136	182	276	93.6	195	76.5	79.4	68.8
23	Lagrangian	469	219	278	590	154	296	120	109	107

Table 6. Percentage deviations in the fit values of B_0 for the HPI from those of B_0 from experiment, denoted by D_3 in the text.

	2-parameter EOS	Ag	Al	Cu	Mg	Mo	Pd	W	MgO	NaCl
1	Bose Roy–Bose Roy*	1.43	3.64	−1.46	−1.45	0.83	1.66	0.88	−1.99	0.15
2	Bose Roy–Bose Roy	0.00	4.61	−2.55	−0.26	0.94	0.28	1.01	−2.76	5.56
3	Born–Mie	−0.29	4.39	−2.47	−1.80	1.21	0.50	1.49	−2.37	6.15
4	Pack–Evans–James	−0.57	4.19	−2.55	−2.21	1.06	0.39	1.39	−2.31	6.15
5	Walzer–Ullmann–Pan'kov	−2.39	3.65	−3.78	−2.64	0.83	−1.16	1.10	−2.88	5.39
6	Born–Mayer	−2.58	2.48	−4.22	−4.24	−0.45	−1.33	0.06	−3.33	4.85
7	Birch–Murnaghan	−3.44	3.95	−3.78	−2.38	0.49	−1.88	0.91	−2.69	5.68
8	Deng–Yan	−2.58	2.48	−4.22	−4.24	−0.45	−1.33	0.06	−3.33	4.85
9	Parsafar-Mason	−1.62	1.04	−3.57	−6.33	−3.39	−0.55	−2.30	−3.40	4.76
10	Holzapfel	−4.88	2.28	−5.60	−4.33	−0.15	−3.21	0.29	−3.72	4.22
11	Grover–Getting–Kennedy	−4.20	1.23	−5.31	−6.19	−1.43	−2.38	−0.62	−3.65	4.34
12	Kunc–Loa–Syassen	−5.62	1.35	−6.26	−5.55	−1.09	−3.82	−0.52	−4.17	3.63
13	Slater–Morse	−5.47	0.96	−6.26	−6.07	−1.62	−3.71	−0.94	−4.29	3.50
14	Davydov	−5.75	1.23	−6.40	−5.69	−1.21	−3.93	−0.58	−4.23	3.59
15	Bardeen	−9.73	2.41	−7.79	−4.01	0.45	−6.86	0.75	−4.10	3.63
16	Shanker–Kushwah–Kumar	−6.27	−0.12	−6.99	−7.64	−2.53	−4.20	−1.62	−4.62	3.00
17	Rydberg	−6.35	0.40	−6.91	−6.77	−2.07	−4.42	−1.30	−4.62	3.08
18	Brennan–Stacey	−6.90	−0.80	−7.57	−8.40	−3.20	−4.81	−2.27	−5.06	2.45
19	Dodson	−16.2	−4.68	−13.6	−13.7	−5.96	−12.2	−4.54	−7.37	−1.03
20	Davis–Gordon	−19.1	−2.18	−14.3	−9.91	−2.60	−14.4	−1.91	−6.92	−0.61
21	Poirier–Tarantola	−21.3	−4.60	−16.2	−13.3	−5.09	−16.2	−3.92	−7.95	−2.16
22	Onat–Vaisnys	−50.7	−28.3	−38.8	−49.1	−28.6	−40.3	−23.2	−19.2	−20.1
23	Lagrangian	−62.9	−39.0	−48.4	−66.6	−40.3	−50.3	−32.5	−24.0	−28.3

Table 7. Percentage deviations in the fit values of B_0' for the HPI from those of B_0' from experiment, denoted by D_4 in the text.

2-parameter EOS	Ag	Al	Cu	Mg	Mo	Pd	W	MgO	NaCl
1 Bose Roy–Bose Roy*	−4.41	−9.60	−6.38	−0.53	−3.08	−1.02	−1.80	−0.53	2.47
2 Bose Roy–Bose Roy	−2.04	−11.4	−4.19	−2.81	−3.33	1.77	−2.15	1.88	−10.5
3 Born–Mie	−2.62	−12.48	−5.28	−2.21	−5.38	0.55	−4.45	0.11	−12.2
4 Pack–Evans–James	−2.86	−12.54	−5.62	−1.97	−5.38	0.09	−4.58	−0.40	−12.7
5 Walzer–Ullmann–Pan'kov	2.80	−10.5	−1.35	0.12	−4.13	5.45	−3.20	2.50	−10.0
6 Born–Mayer	2.66	−7.71	−0.53	4.11	−0.43	5.38	0.10	3.98	−8.53
7 Birch–Murnaghan	5.88	−11.3	−1.22	−0.60	−3.25	7.70	−2.60	1.59	−10.9
8 Deng–Yan	9.87	1.57	7.24	14.7	11.0	12.9	11.5	13.4	−0.23
9 Parsafar-Mason	0.81	−4.62	−2.04	8.51	7.18	3.74	6.90	4.42	−8.14
10 Holzapfel	9.48	−6.80	3.98	4.93	−1.18	11.5	−0.40	6.13	−6.50
11 Grover–Getting–Kennedy	4.14	−6.29	0.42	6.92	0.85	6.17	0.93	3.98	−8.38
12 Kunc–Loa–Syassen	11.5	−4.22	5.98	8.44	1.88	13.3	2.35	7.99	−4.72
13 Slater–Morse	10.9	−3.22	5.92	9.83	3.45	12.9	3.75	8.41	−4.32
14 Davydov	11.8	−3.90	6.30	8.85	2.18	13.7	2.63	8.25	−4.47
15 Bardeen	27.3	−6.95	12.4	4.30	−3.03	25.7	−2.03	8.08	−4.50
16 Shanker–Kushwah–Kumar	11.3	−1.33	6.78	13.0	5.33	13.1	5.25	9.09	−3.54
17 Rydberg	13.4	−1.63	7.96	11.9	4.90	15.2	5.10	9.82	−2.94
18 Brennan–Stacey	13.5	1.21	8.93	16.0	8.33	15.2	8.15	11.3	−1.45
19 Dodson	46.4	14.3	31.3	35.3	18.2	42.6	16.9	22.8	10.5
20 Davis–Gordon	71.0	9.19	41.2	26.5	8.25	61.3	8.60	23.3	11.4
21 Poirier–Tarantola	81.6	17.8	49.4	39.8	17.4	69.7	16.6	28.8	17.2
22 Onat–Vaisnys	367	159	222	338	158	268	131	110	115
23 Lagrangian	634	268	350	743	278	418	217	157	181

of magnitude. With similar exercises for all the EOSs considered, we thus have a table in which the deviation points are spread over nine columns following the column of EOSs. One might immediately suggest, following a traditional path, that the magnitude of the DPs in the ninth column may be chosen as a marker to scale the adequacy of the EOSs. To elaborate, the EOS with the lowest relative mismatch, i.e. with the lowest magnitude of D_i in the ninth column may be credited with an integer 1, and the EOSs with successively higher numerical values of the D_i/RMSD may be discredited with successively higher integers, increasing by unity. It may be emphasized here that the numerical values assigned to the EOSs merely denote their adequacy on a relative scale—the higher the numerical values the lower the adequacy. However, the crux of the problem of this one-step CIA is that the D_i's are not in general consistent in their magnitude. This non-uniformity factor may be appreciated by focusing attention on the D_1s in the first row of table 4, where as many as seven deviation points remain well within 0.5, while the ninth (the largest one) jumps to as much as 1.32. Similarly, turning to the D_2s in the first row of table 5, while as many as seven D_2s remain within 3; the ninth, the largest, jumps to as high as 10.1. Obviously, using the largest value as a marker is quite unlikely to yield an infallible inference. To resolve this problem, we have to follow a path that must be unbiased and at the same must be capable of incorporating the inconsistency features of the deviation points. Further, it must be pointed out that statistically we have to consider at least five out of the nine deviation points for each EOS. To this end, therefore, we have considered the deviation points in columns 5, 6, 7, 8 and 9, separately. The EOSs are marked with integers depending on the relative magnitude of the deviation points in columns 5 to 9, separately. Each EOS thus has a set of five integers, denoting its relative adequacy corresponding to each column. These integers are summed up and then averaged over five columns by dividing by 5, and the average

Table 8. Number of wiggles of the data deviation curves about the fits (NW).

	2-parameter EOS	Ag	Al	Cu	Mg	Mo	Pd	W	MgO	NaCl	RA
1	Bose Roy–Bose Roy*	15	11	24	13	12	17	11	24	17	1
2	Bose Roy–Bose Roy	2	2	5	2	12	2	9	5	2	2
3	Born–Mie	2	5	3	2	7	2	5	7	2	3
4	Pack–Evans–James	2	5	3	2	5	2	5	7	2	4
5	Walzer–Ullmann–Pan'kov	2	9	2	2	5	2	5	5	2	5
6	Birch–Murnaghan	2	5	2	2	4	2	5	5	2	6
7	Bardeen	2	6	2	2	6	2	2	2	2	7
8	Born–Mayer	2	6	2	2	2	2	2	5	2	8
9	Deng–Yan	2	6	2	2	2	2	2	5	2	8
10	Holzapfel	2	4	2	2	4	2	4	2	2	9
11	Dodson	2	2	2	2	2	2	2	2	13	10
12	Poirier–Tarantola	2	2	2	2	2	2	2	2	13	10
13	Davis–Gordon	2	2	2	2	2	2	2	2	9	11
14	Kunc–Loa–Syassen	2	2	2	2	2	2	2	2	2	12
15	Slater–Morse	2	2	2	2	2	2	2	2	2	12
16	Parsafar–Mason	2	2	2	2	2	2	2	2	2	12
17	Rydberg	2	2	2	2	2	2	2	2	2	12
18	Davydov	2	2	2	2	2	2	2	2	2	12
19	Grover–Getting–Kennedy	2	2	2	2	2	2	2	2	2	12
20	Shanker–Kushwah–Kumar	2	2	2	2	2	2	2	2	2	12
21	Brennan–Stacey	2	2	2	2	2	2	2	2	2	12
22	Onat–Vaisnys	2	2	2	2	2	2	2	2	2	12
23	Lagrangian	2	2	2	2	2	2	2	2	2	12

numerical values are then again marked with integers, to denote the overall relative adequacy against the test parameter. It will be interesting to note that if we consider all the nine columns separately we arrive at the same overall relative adequacy of the EOSs as obtained considering only five columns in line with the CIA, shown in table 12.

In the second approach, called the individual isotherm approach (IIA), the responses of the EOSs towards the individual isotherms is incorporated in scaling their relative adequacy. In the IIA, the EOSs are marked with integers depending on the relative magnitude of the DPs against each isotherm. For each EOS, nine integers thus obtained for the nine isotherms are added and averaged over nine isotherms, and the average numerical values are again changed to integers denoting the relative adequacy of the EOSs, as discussed above. In principle, if the deviation points inferred from an EOS for all the isotherms are equal in magnitude, the two approaches CI and II lead to the concurrent conclusions, irrespective of the number of isotherms considered. In practice, however, if the DPs inferred from an EOS are appreciably consistent when considered on an overall basis, the two approaches would have an increasing tendency to yield similar inferences as the number of isotherms considered increases. Tables 9 and 10 illustrate the two approaches with reference to the assessment of the relative adequacy of the EOSs for D_1.

3.2. Departure of the data deviation plot from the normal error curve and adequacy of EOS

As dealt with at length in our previous study [14], the curve-fitting capability of the EOSs can be compared on the basis of the departure of the data deviation curves from the ideal normal random variable curve. In general, the higher the number of wiggles of the data deviation curves about the fits, the higher is the relative adequacy of an EOS. If two EOSs differ

Table 9. Individual isotherm approach (IIA) illustrated with reference to the adequacy of D_1. RA denotes relative adequacy.

	2-parameter EOS	Ag	Al	Cu	Mg	Mo	Pd	W	MgO	NaCl	Av.	RA
1	Bose Roy–Bose Roy*	1	8	1	1	7	1	7	1	1	3.11	1
2	Bose Roy–Bose Roy	2	9	3	3	3	4	4	5	17	5.56	2
3	Born–Mie	3	7	2	2	4	2	8	3	20	5.67	3
4	Pack–Evans–James	4	6	4	4	2	3	6	2	19	5.56	2
5	Walzer–Ullmann–Pan'kov	6	3	8	6	1	6	3	6	16	6.11	4
6	Born–Mayer	7	1	9	8	9	7	9	7	15	8	6
7	Birch–Murnaghan	8	5	8	5	5	8	2	4	18	7	5
8	Deng–Yan	7	1	9	8	9	7	9	7	15	8	6
9	Parsafar–Mason	5	13	5	14	18	5	17	8	14	11	10
10	Holzapfel	10	4	11	9	8	10	5	10	13	8.89	7
11	Grover–Getting–Kennedy	9	12	10	13	13	9	12	9	12	11	10
12	Kunc–Loa–Syassen	12	10	12	10	10	12	10	12	10	10.89	9
13	Slater–Morse	11	14	12	12	12	11	13	14	8	11.89	12
14	Davydov	13	11	13	11	11	13	11	13	9	11.67	11
15	Bardeen	17	2	16	7	6	17	1	11	11	9.78	8
16	Shanker–Kushwah–Kumar	15	16	15	16	16	14	15	16	6	14.33	14
17	Rydberg	14	15	14	15	14	15	14	15	7	13.67	13
18	Brennan–Stacey	16	17	16	17	17	16	18	17	5	15.44	15
19	Dodson	18	20	18	20	20	18	20	19	3	17.33	17
20	Davis–Gordon	19	18	19	18	15	19	16	18	2	16.00	16
21	Poirier–Tarantola	20	19	20	19	19	20	19	20	4	17.78	18
22	Onat–Vaisnys	21	21	21	21	21	21	21	21	21	21	19
23	Lagrangian	22	22	22	22	22	22	22	22	22	22	20

significantly from each other with regard to their curve-fitting capability, it would be manifest in the significant difference in the number of the wiggles (NW) of their data deviation curves. If, however, the difference is not very significant, or marginal, the same may be reflected in the marginal difference in the number of wiggles; or merely in the degree of departures of their data deviation curves from the symmetric normal random distribution pattern, and an explicit difference in the number of wiggles may not be registered. In order to assess any significant difference in the fitting capability of the compared EOSs, we have plotted the deviation in the response, P, against the regressor, V/V_0, inferred from all the EOSs for all the nine isotherms considered, and counted the number of times the data deviation curves cross the fit. The enumerated numerical values are tabulated in table 8. It may be noted that the numerical values of NW are so arranged that, on an overall basis, in any row the number of isotherms, for which a higher number of wiggles is inferred from an EOS, is higher than those that follow down the table.

Table 8 shows that for all the nine isotherms considered there is a wide difference between the number of wiggles (NW) inferred from our three-parameter EOS, and the rest of the 21 two-parameter EOSs compared. It is important to note that even our two-parameter EOS is overall better randomized compared to the other two-parameter EOSs.

3.3. Results and discussions

Table 12, in conjunction with tables 3–8 and 11 depicts the overall position of the EOSs with regard to their relative curve-fitting capability. In table 12, the relative performance of the individual EOSs against the six tests—the fitting accuracy, stability of the fit parameters B_0 and

Table 10. Collective isotherm approach (CIA) illustrated with reference to the adequacy of D_1. A, B, C, D and E denote the fifth, sixth, seventh, eighth and ninth columns, respectively, as referred to in the text.

	2-parameter EOS	A	B	C	D	E	Av.	RA
1	Bose Roy–Bose Roy*	1	1	1	1	1	1	1
2	Bose Roy–Bose Roy	4	3	2	3	4	3.2	2
3	Born–Mie	2	2	4	2	9	3.8	3
4	Pack–Evans–James	3	4	3	4	8	4.4	4
5	Walzer–Ullmann–Pan'kov	6	5	5	5	3	4.8	5
6	Born–Mayer	6	5	5	5	3	4.8	5
7	Birch–Murnaghan	5	5	6	9	5	6	7
8	Deng–Yan	7	6	7	6	2	5.6	6
9	Parsafar–Mason	8	7	8	7	7	7.4	8
10	Holzapfel	13	10	10	8	10	10.2	9
11	Grover–Getting–Kennedy	17	9	9	13	6	10.8	10
12	Kunc–Loa–Syassen	15	11	11	10	12	11.8	11
13	Slater–Morse	12	12	13	11	11	11.8	11
14	Davydov	14	13	12	12	13	12.8	12
15	Bardeen	10	8	17	17	17	13.8	14
16	Shanker–Kushwah–Kumar	11	15	14	15	15	14	15
17	Rydberg	9	14	15	14	14	13.2	13
18	Brennan–Stacey	16	16	16	16	16	16	16
19	Dodson	20	18	18	18	18	18.4	18
20	Davis–Gordon	18	17	18	19	19	18.2	17
21	Poirier–Tarantola	19	19	19	20	20	19.4	19
22	Onat–Vaisnys	21	20	20	21	21	20.6	20
23	Lagrangian	22	21	21	22	22	21.6	21

B_0', agreement of the fit parameters B_0, and B_0' with experiment, and randomization of the data points about the fits (NW)—is expressed in terms of the numerical values denoting their relative adequacy with reference to their individual responses to the said tests in tables 3–8, taking recourse to both the individual and collective isotherm approaches. It must be emphasized that these numerical values do not constitute any quantitative scale. They simply indicate that the higher the numerical value, the lower is the rating against the tests specified at the column heads, on a relative scale. One can note in tables 3–8 that our three-parameter model (equation (33)) is, in general, superior to the nearest rival, which interestingly happens to be our two-parameter EOS (equation (34)), on all the six tests—but the difference between the successive EOSs, down the tables, increases slowly thereafter, and the worst ones appear at the bottom of the table. It must be emphasized here that all the six tests are highly correlated, and none of them alone is sufficient to assess the adequacy of an EOS.

Table 12 shows clearly that the overall positions of relative adequacy suggested by the two approaches, CIA and CIIA, accord well for the best seven EOSs, down to the Birch EOS; implying thereby that the number of isotherms considered for comparison purposes is adequate, statistically, for a meaningful discrimination between the EOSs. Good consistency however, should not be misconstrued as a measure of good adequacy—to illustrate this the two approaches concur even for the worst three EOSs at the bottom of the table. Relative adequacy inferred from the two approaches is in conflict for the pair of EOSs like the Slater–Morse and the Davydov, the Shanker–Kushwah–Kumar and the Rydberg and the Dodson and the Davis–Gordon. As such, we cannot argue that either one or the other of these pairs of EOSs fits the isotherms better.

Table 11. Overall relative adequacy (ORA) of the EOSs based on their relative performances against the six tests as shown in tables 3–8, using the individual isotherm approach.

	2-parameter EOS	RMSD	D1	D2	D3	D4	NW	ORA
1	Bose Roy–Bose Roy*	1	1	4	1	2	1	1
2	Bose Roy–Bose Roy	2	2	1	2	5	2	2
3	Born–Mie	3	3	3	5	9	3	3
4	Pack–Evans–James	4	2	2	4	11	4	4
5	Walzer–Ullmann–Pan'kov	5	4	3	7	6	5	5
6	Born–Mayer	7	6	6	3	1	8	6
7	Birch–Murnaghan	6	5	5	8	7	6	7
8	Holzapfel	8	7	7	6	4	9	8
9	Deng–Yan	9	6	4	3	17	8	9
10	Grover–Getting–Kennedy	14	10	10	9	3	12	10
11	Bardeen	10	8	9	14	14	7	11
12	Kunc–Loa–Syassen	11	9	11	10	10	12	12
13	Parsafar–Mason	15	10	8	11	8	12	13
14	Davydov	13	11	12	12	13	12	14
15	Slater–Morse	12	12	13	13	12	12	15
16	Rydberg	10	13	14	15	16	12	16
17	Shanker–Kushwah–Kumar	16	14	15	16	15	12	17
18	Brennan–Stacey	17	15	16	17	18	12	18
19	Davis–Gordon	18	16	17	18	19	11	19
20	Dodson	19	17	18	19	20	10	20
21	Poirier–Tarantola	20	18	19	20	21	10	21
22	Onat–Vaisnys	21	19	20	21	22	12	22
23	Lagrangian	22	20	21	22	23	12	23

Our three-parameter EOS best fits the data curves; and more importantly, since its two-parameter counterpart generally duplicates the data curves better than all the two-parameter EOSs considered, asserts the robustness of our original three-parameter model. The most noticeable feature of the results in table 12, however, is that the old quantum-based Pack–Evans–James model, which now is virtually lost to oblivion, not attracting even a passing mention in the current literature, as well as the old lattice-potential based Born–Mie EOS, do fit the isotherms significantly better than the Birch–Murnaghan EOS. Hence the use of the Birch EOS as a standard EOS in the literature in curve-fitting purposes, for over half a century now—especially when EOSs with a decisively higher fitting accuracy already existed—is not justified.

The EOS model of Deng and Yan (equation (31)), based on the Born–Mayer model, has proved counterproductive in that the original Born–Mayer EOS fits the data curves better than their model. Similarly, the Shanker–Kushwah–Kumar EOS which is based on a combined form of an inverse power dependence (Born–Mie EOS) and exponential dependence (Born–Mayer EOS), is also counterproductive—because both the Born–Mie and the Born–Mayer EOSs are in significantly better agreement with the compression curves than the Shanker–Kushwah–Kumar EOS.

In sharp contrast with the assertion of Oganov *et al* [103], and in line with the conclusions of Schlosser *et al* [104], Cohen *et al* [105] and Hama *et al* [106] that the Rydberg EOS is the best EOS formulation available, giving the best fit of experimental data over the full range of compressions experimentally available, one can appreciate from table 12 (and tables 3–8) that this conclusion is far from truth insofar as the accuracy in curve-fitting capability is considered.

Table 12. Overall relative adequacy (ORA) of the EOSs based on their relative performances against the six tests as shown in tables 3–8, using the collective isotherm approach.

	2-parameter EOS	RMSD	D1	D2	D3	D4	NW	ORA (CIA)	ORA (IIA)
1	Bose Roy–Bose Roy*	1	1	1	1	1	1	1	1
2	Bose Roy–Bose Roy	2	2	6	2	3	2	2	2
3	Born–Mie	3	3	4	3	8	3	3	3
4	Pack–Evans–James	5	4	2	2	9	4	4	4
5	Walzer–Ullmann–Pan'kov	4	5	5	4	4	5	5	5
6	Born–Mayer	7	6	7	5	2	8	6	6
7	Birch–Murnaghan	6	7	9	6	7	6	7	7
8	Deng–Yan	7	6	3	5	16	8	8	9
9	Parsafar-Mason	10	8	8	7	6	12	9	13
10	Holzapfel	8	9	11	8	9	9	10	8
11	Grover–Getting–Kennedy	13	10	10	9	5	12	11	10
12	Kunc–Loa–Syassen	9	11	12	10	10	12	12	12
13	Slater–Morse	11	11	13	11	11	12	13	15
14	Davydov	12	12	14	12	12	12	14	14
15	Bardeen	14	14	16	13	14	7	15	11
16	Shanker–Kushwah–Kumar	16	15	15	14	13	12	16	17
17	Rydberg	15	13	17	14	15	12	17	16
18	Brennan–Stacey	17	16	18	15	17	12	18	18
19	Dodson	19	18	19	16	18	10	19	20
20	Davis–Gordon	18	17	20	17	19	11	20	19
21	Poirier–Tarantola	20	19	21	18	20	10	21	21
22	Onat–Vaisnys	21	20	22	19	21	12	22	22
23	Lagrangian	22	21	23	20	22	12	23	23

Because the position of the Rydberg EOS, on the scale of relative curve-fitting adequacy, is as low as 17, and as many as nine two-parameter EOSs had already appeared in the literature much before the Rydberg. Further, both the two- and three-parameter Rydberg EOSs prove an utter failure in duplicating Nellis *et al*'s data curve of Cu [89] ranging to the terapascal regime. The Rydberg EOS has currently attracted undue attention because of the claim of Vinet and co-workers that it is a universal EOS. In fact any proposal to project the two-parameter Rydberg EOS as a universal one represents a lack of knowledge or a lack of attention to the experimental facts [107, 108].

The claim of Parsafar and Mason, that their EOS describes the data curve more accurately than the Rydberg EOS, is well substantiated on experimental grounds. One notes from table 12 that among the two-parameter EOSs compared, the Parsafar and Mason EOS ranks eighth on the scale of relative adequacy, (table 12) as compared to sixteenth for the latter. The Holzapfel EOS, resulting from the grafting of the Thomas–Fermi limiting condition into the Rydberg EOS, does exhibit a decisive superiority in curve-fitting compared to the Rydberg EOS, on all the six counts of the composite test. The adequacy of the Kunc–Loa–Syassen EOS, as expected, lies between those of the Holzapfel and the Rydberg EOS, of which it is a hybrid.

The Morse potential continues to be widely used in theoretical thermodynamic studies of solids [109–113] unlike the Rydberg potential—although the latter was considered better in the explanation of diatomic spectra. And interestingly, the Slater–Morse EOS proves better in curve-fitting than the Rydberg EOS. The apparent poor performance of the Bardeen EOS, based on quantum-mechanical calculations, is understandable. In principle, the limitations on accuracy in the quantum-mechanical calculations of an equation of state are set only

by mathematical complications in the solution of Schrödinger's equation for the many-body problem. And the original derivation of this equation from quantum mechanics applies specifically to alkali metals. The poor performance of the Brennan–Stacey EOS, apparently based on a clear thermodynamic argument, has its genesis in the facts that both the free volume formula and the assumption $\gamma\rho$ = constant are flawed; the authors realizing these inadequacies in their later study, based on molecular dynamics [114, 115]. And as such, equation (25) should be viewed merely as an empirical model. The discouraging performance of the Dodson equation, seemingly based on well-founded theoretical observations of Moruzzi *et al*, is probably due to its origin anchored in presumptions that have no physical significance as the rough model of Moruzzi *et al* for electron density versus bulk compressibility has been used far outside its regime of applicability [61]. The Lagrangian EOS as well as the Davis–Gordon and the Onat–Vaisnys EOSs do not fit the data curves well because of their poor convergence. The Lagrangian EOS, positioned at the lowest position of the scale of relative adequacy, allows an easy appreciation of the relative accuracy achieved by the rest of the EOSs compared. The argument underlying the formulation of the Poirier–Tarantola EOS is appealing and compelling [80]. But it flounders on the test bed of experiment, appearing in table 12 along with the worst performers. Thus the Poirier and Tarantola EOS best illustrates the dictum that the real test of the adequacy of an EOS is its agreement with experiment, i.e. nature, and not the apparent appeal of its underlying argument.

Figures 1(a)–7(c) compare and examine the deviations between the data points and data fits with various equations, and reinforce our earlier conclusions based on numerical results. One important feature, which is conspicuous in all the graphs, is that the fits yielded by equation (33) result in a very accurate representation of the data. The magnitude of systematic deviations at low pressure is appreciably low—a characteristic of a well-behaved EOS that helps in the extraction of accurate values of fit parameters [116], and is much lower than those arising from all the other EOSs. And randomization of the data points about the fits is also decisively better—the deviation curves hovering closely around the fits, over the entire pressure range. In general, the deviation curves for equation (34) follow those for equation (33) more closely than the rest of the EOSs. Overall, the graphs show that the difference in the curve-fitting capability between the EOSs (33) and (34), is not as pronounced as the difference between them and the rest of the EOS models.

A few comments may be made with regard to the status of the Birch–Murnaghan model, used as a standard EOS in the field of EOS. The Birch EOS is neither unique nor exact; neither its physical behaviour is impeccable nor its theoretical bases above criticism [37, 39, 40, 106, 117–121]. Further, neither is acceptable for the accurate representation of the high-precision low-compression data [116], nor are its two- and three-parameter EOS forms in accurate agreement with the ultra-high-pressure model-independent compression regime [89]. Additionally, neither is it compatible with the recent theoretical study [122], nor is its curve-fitting capability the best compared to the rest of the then existing EOSs (table 12). Yet it has been widely used for curve-fitting purposes for over a half a century now [4, 5, 123, 124]—Why? It is probably because Birch pioneered the interpretation of seismological observations of the deep Earth. The apparent success being attributed to the in-built constraint of its relation, giving in its simplest form $B_0' = 4$, which happens to be a good average for many minerals studied. The Birch analysis was so persuasive that most geophysicists have followed his lead without contemplating alternative approaches. However, the present study indicates unambiguously that two viable alternative EOSs, the Born–Mie and the Pack–Evans–James, with a significantly better accuracy in curve-fitting, already existed. And therefore, the use of the Birch relation for the curve-fitting of the compression data cannot be justified either in the present or in the past.

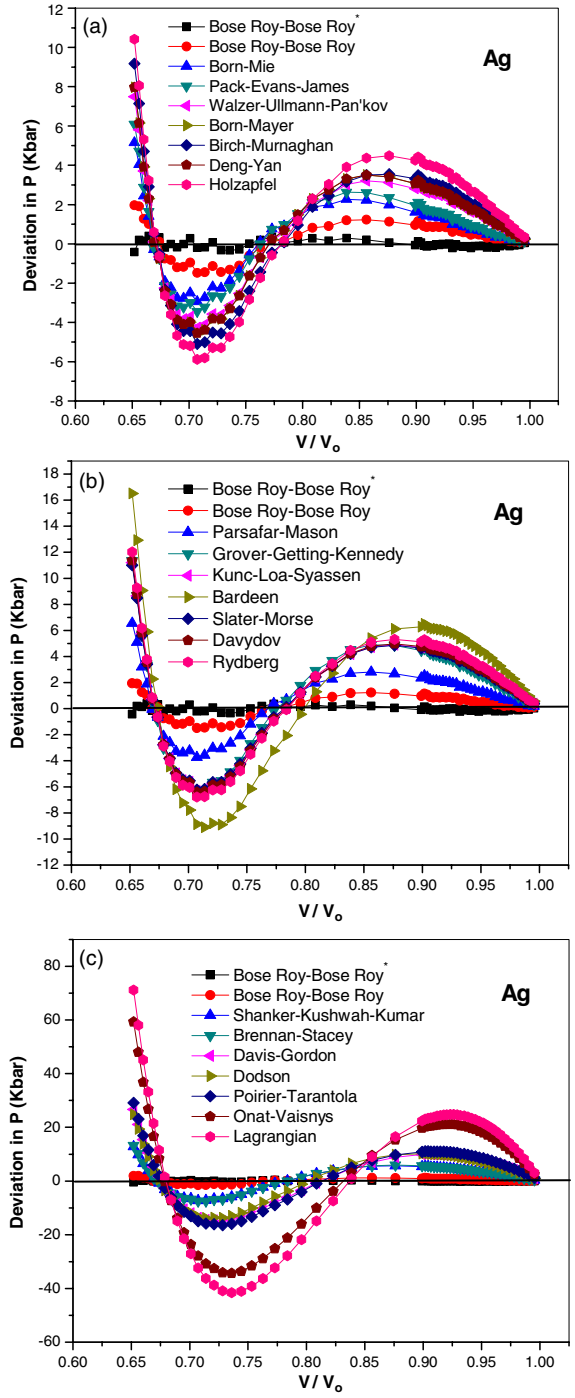

Figure 1. (a)–(c). Comparison of deviations between the data curve of Ag [86] and the fits from Bose Roy–Bose Roy*, and the other equations of state.

4. Summary

The EOS discrimination technique is rendered more stringent in the present study. Following an unbiased discrimination technique—the harshest ever designed and applied in the literature—

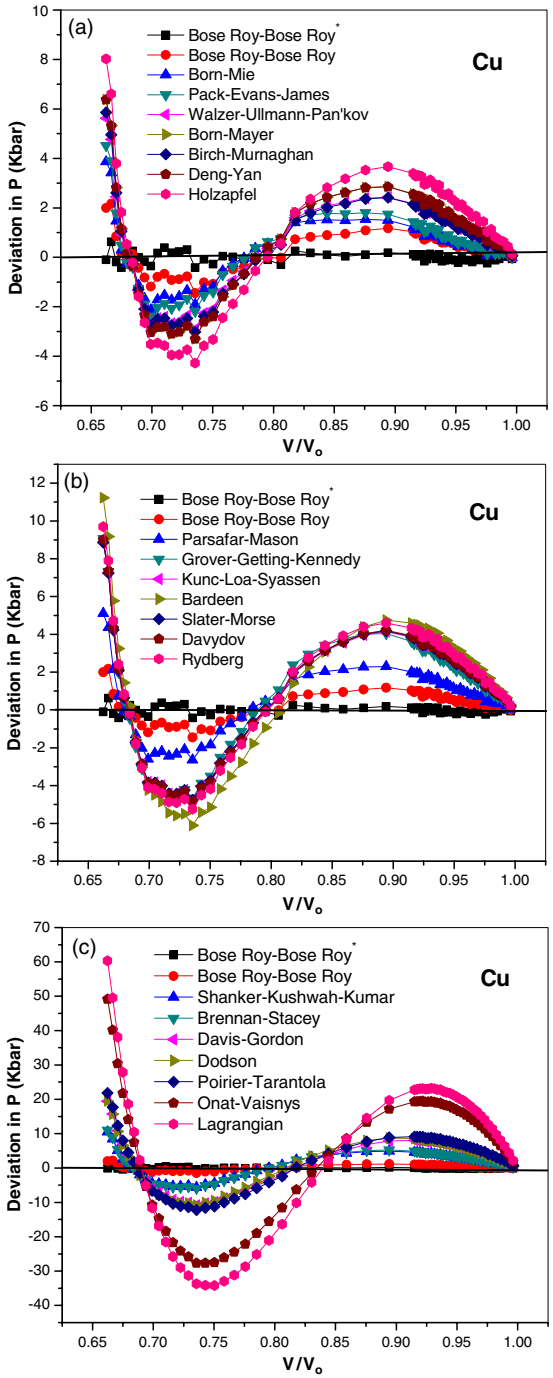

Figure 2. (a)–(c). Comparison of deviations between the data curve of Cu [86] and the fits from Bose Roy–Bose Roy*, and the other equations of state.

the curve-fitting capability of as many as 21 isothermal unrealistic two-parameter EOSs has been assessed on an individual as well as a comparative basis—and compared with our realistic

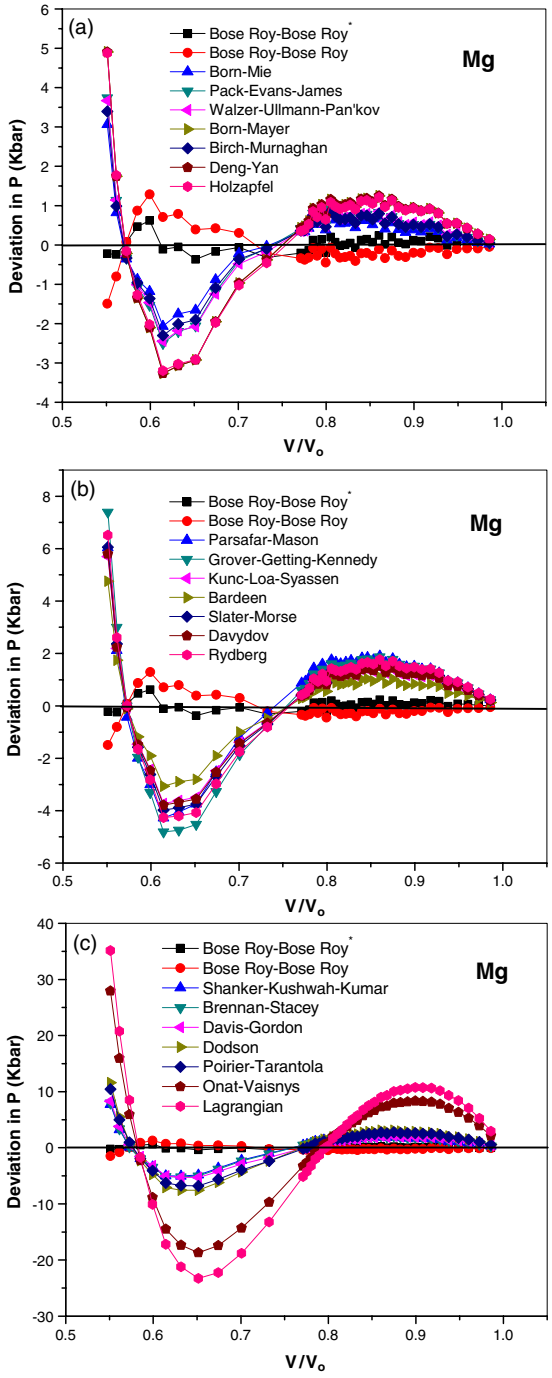

Figure 3. (a)–(c). Comparison of deviations between the data curve of Mg [86] and the fits from Bose Roy–Bose Roy*, and the other equations of state.

three- and two-parameter EOSs. It is shown that there is no justification whatsoever in the use of the Birch–Murnaghan EOS and the Rydberg EOS in the curve-fitting of the compression

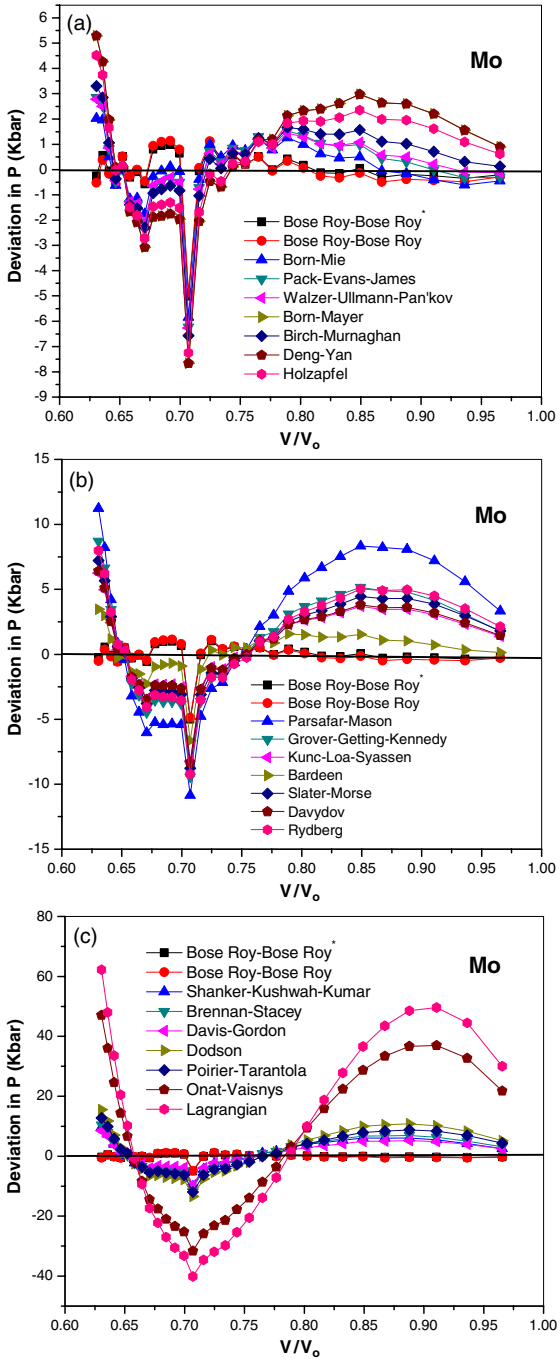

Figure 4. (a)–(c). Comparison of deviations between the data curve of Mo [88] and the fits from Bose Roy–Bose Roy*, and the other equations of state.

data. The Birch–Murnaghan approach, which continues to be unjustifiably used for over a half a century now in the curve-fitting of the laboratory compression data, must be judged not

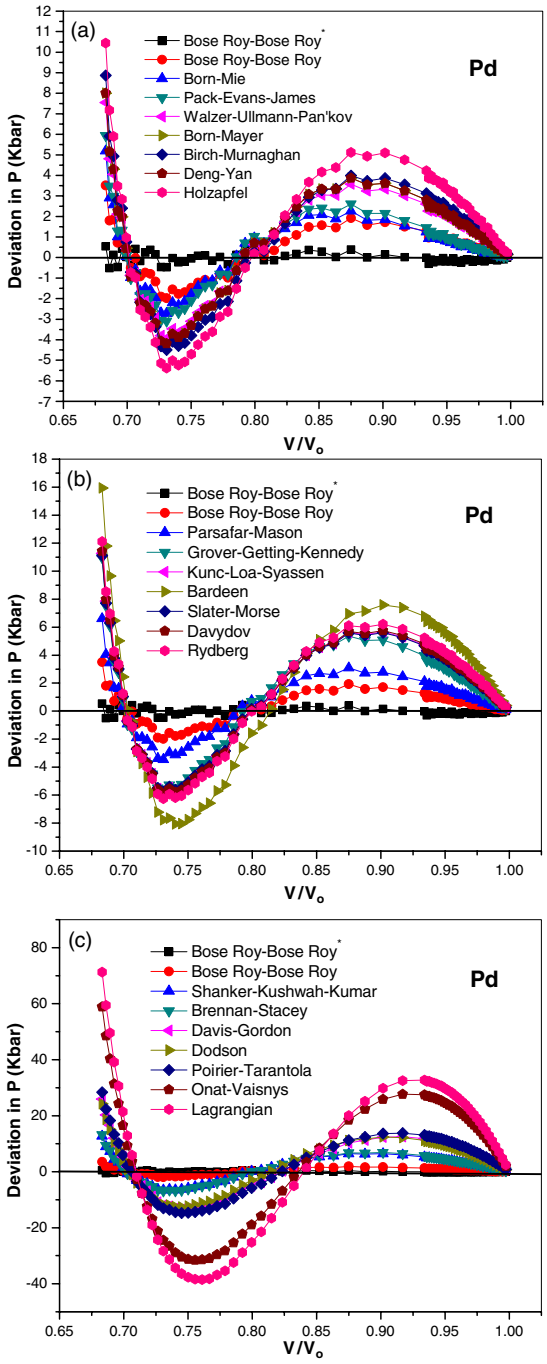

Figure 5. (a)–(c). Comparison of deviations between the data curve of Pd [86] and the fits from Bose Roy–Bose Roy*, and the other equations of state.

by its pedigree but by the accuracy of its response to observations, as for any other empirical relationship. Likewise, the current use of the Rydberg EOS—with a much poorer performance

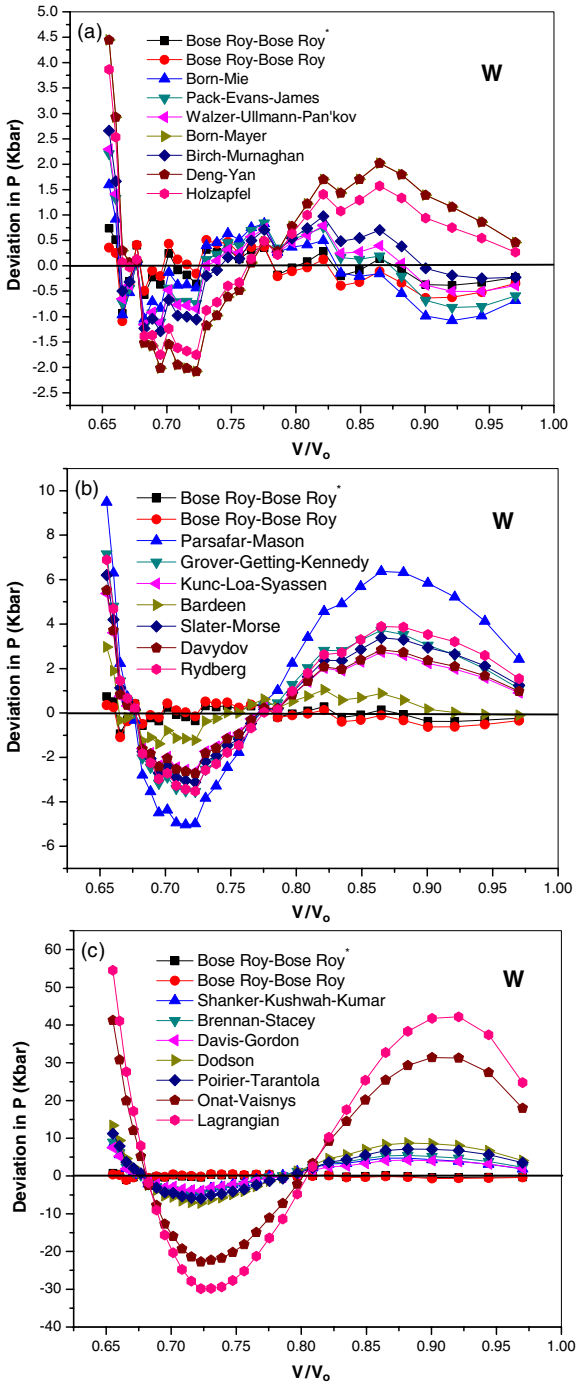

Figure 6. (a)–(c). Comparison of deviations between the data curve of W [88] and the fits from Bose Roy–Bose Roy*, and the other equations of state.

compared to the Birch EOS—as a standard EOS in the curve-fitting exercises, is also unfounded on experimental grounds. Conflicting conclusions, widespread in the literature, regarding the

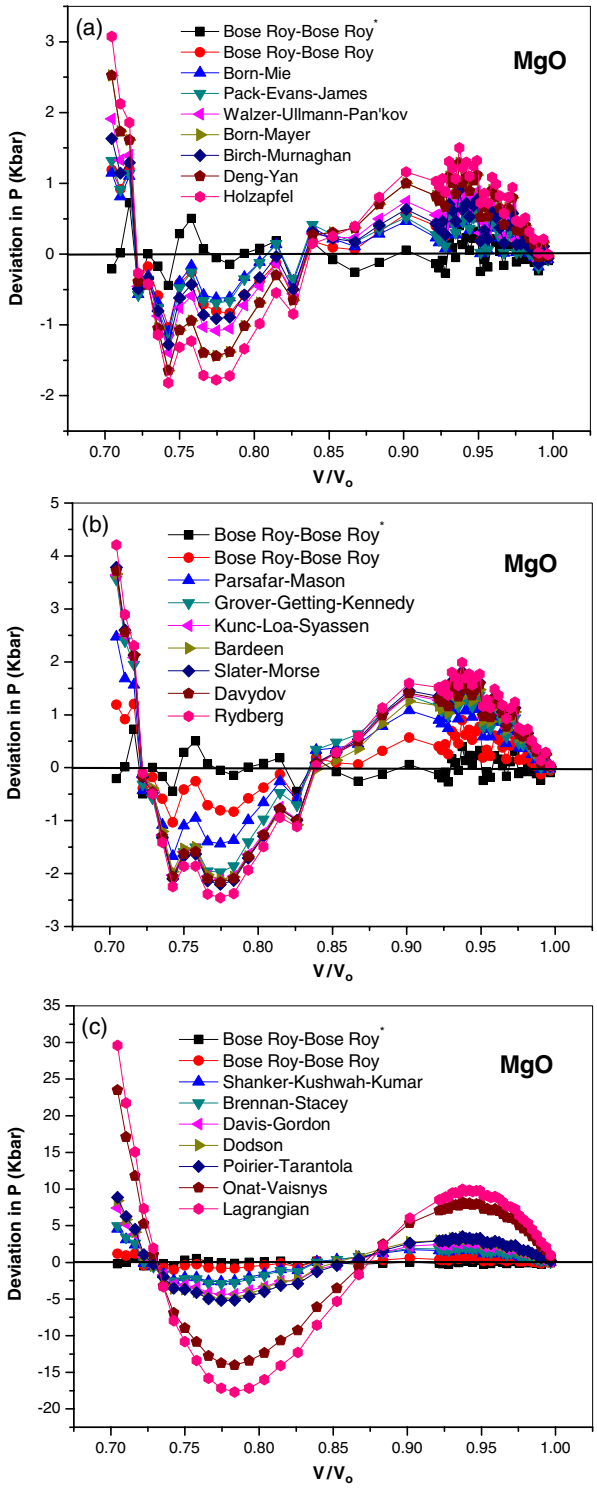

Figure 7. (a)–(c). Comparison of deviations between the data curve of MgO [86] and the fits from Bose Roy–Bose Roy*, and the other equations of state.

relative curve-fitting utility of the isothermal unrealistic two-parameter EOSs, arising from an inappropriate and inadequate methods used for EOS discrimination, are set to rest. On an overall assay, it transpires that in general the curve-fitting predictions based on the two-parameter EOSs are fraught with a higher level of uncertainty compared to the three-parameter ones. Further, it is shown that the overall curve-fitting capability of our two-parameter EOS is superior to all the unrealistic two-parameter EOSs considered. To conclude, our three-parameter EOS is decisively superior not only to all the three-parameter EOSs but also to all the unrealistic two-parameter EOSs thus far proposed in the literature.

References

[1] Cheng D, Wang S and Ye H 2001 *Phys. Rev.* B **64** 024107
[2] Hanfland M, Loa I and Syassen K 2002 *Phys. Rev.* B **65** 184109
[3] Karasevskii A I and Holzapfel W B 2003 *Phys. Rev.* B **67** 224301
[4] Luo S N, Swift D C, Mulford R N, Drummond N D and Ackland G J 2004 *J. Phys.: Condens. Matter* **16** 5435
[5] Wang S Q, Ye H Q and Yip S 2006 *J. Phys.: Condens. Matter* **18** 395
[6] Katahara K W, Manghnani M H, Ling L C and Fisher E S 1997 *High Pressure Research Applications in Geophysics* ed M H Manghnani and S-I Akimoto (New York: Academic) p 351
[7] Yourdshahyan Y, Ruberto C, Bengtsson L and Lundqvist B I 1997 *Phys. Rev.* B **56** 8553
[8] Lundqvist B I, Bogicevic A, Carling K, Dudiy S V, Gao S, Hartford J, Hyldgaard P, Jacobson N, Langreth D C, Lorente N, Ovesson S, Razaznejad B and Yourdshahyan Y 2001 *Surf. Sci.* **493** 253
[9] Cynn H, Klepeis J E, Yoo C-S and Young D A 2002 *Phys. Rev. Lett.* **88** 135701
[10] Ziambaras E and Scroder E 2003 *Phys. Rev.* B **68** 064112
[11] Nellis W J 2006 *Rep. Prog. Phys.* **69** 1479
[12] Chen C Q, Shi Y, Zhang Y S, Zhu J and Yan Y J 2006 *Phys. Rev. Lett.* **96** 075505
[13] Juodkazis S, Nishimura K, Tanaka S, Misawa H, Gamaly E G, Luther-Davis B, Hallo L, Nicolai P and Tikhonchuk V T 2006 *Phys. Rev. Lett.* **96** 166101
[14] Bose Roy P and Bose Roy S 2005 *J. Phys.: Condens. Matter* **17** 6193
[15] Bose Roy S and Bose Roy P 1999 *J. Phys.: Condens. Matter* **11** 10375
[16] Bose Roy P and Bose Roy S 2003 *J. Phys.: Condens. Matter* **15** 1643
[17] Mie G 1903 *Ann. Phys.* **11** 657
[18] Gruneisen E 1912 *Ann. Phys.* **39** 257
[19] Partington J R 1957 *An Advanced Treatise on Physical Chemistry* vol 3 (London: Longmans) p 345
[20] Stacey F D, Brennan B J and Irvine R D 1981 *Geophys. Surv.* **4** 189
[21] Stacey F D and Davis P M 2004 *Phys. Earth Planet. Inter.* **142** 137
[22] Born M 1920 *Ann. Phys., Lpz.* **61** 87
[23] Born M 1939 *J. Chem. Phys.* **7** 591
[24] Anderson O L 1967 *J. Geophys. Res.* **72** 3661
[25] Anderson O L 1970 *J. Geophys. Res.* **75** 2719
[26] Anderson O L 1995 *Equations of State of Solids for Geophysical and Ceramic Science* (NewYork: Oxford University Press)
[27] Walzer U, Ullmann W and Pan'kov V L 1979 *Phys. Earth Planet. Inter.* **18** 1
[28] Ullmann W and Pan'kov V L 1980 *Phys. Earth Planet. Inter.* **22** 194
[29] Born M and Mayer J E 1932 *Z. Phys.* **75** 1
[30] Varshni Y P 1963 *Rev. Mod. Phys.* **35** 130
[31] Tosi M P 1964 *Solid State Phys.* **16** 1
[32] Birch F 1938 *J. Appl. Phys.* **9** 279
[33] Birch F 1939 *Bull. Seis. Soc. Am.* **29** 463
[34] Birch F 1947 *Phys. Rev.* **71** 809
[35] Birch F 1952 *J. Geophys. Res.* **57** 227
[36] Birch F 1978 *J. Geophys. Res.* **83** 1257
[37] Thomsen L 1970 *J. Phys. Chem. Solids* **31** 2003
[38] Davies G F 1973 *J. Phys. Chem. Solids* **34** 841
[39] Truesdell C and Noll W 1965 *The Non-linear Field Theories of Mechanics, Sections* (Berlin: Springer) pp 15–19
[40] Knopoff L 1963 *High Pressure Physics and Chemistry* ed R S Bradley (San Diego, CA: Academic) p 227
[41] Aidun J, Bukowinski M S T and Ross M 1984 *Phys. Rev.* B **29** 2611

[42] Weaver J S 1976 *J. Phys. Chem. Solids* **37** 711
[43] Murnaghan F D 1937 *Am. J. Math.* **59** 235
[44] Murnaghan F D 1951 *Finite Deformation of an Elastic Solid* (New York: Wiley)
[45] Bardeen J 1938 *J. Chem. Phys.* **6** 372
[46] Wigner E and Seitz F 1933 *Phys. Rev.* **43** 804
[47] Wigner E and Seitz F 1934 *Phys. Rev.* **46** 509
[48] Gilvarry J J 1957 *J. Appl. Phys.* **28** 1253
[49] Morse P M 1929 *Phys. Rev.* **34** 57
[50] Varshni Y P 1957 *Rev. Mod. Phys.* **29** 664
[51] Slater J C 1939 *Introduction to Chemical Physics* (New York: McGraw-Hill) p 521
[52] Rydberg R 1932 *Z. Phys.* **73** 376
[53] Rose J H, Smith J R, Guinea F and Ferrante J 1984 *Phys. Rev.* B **29** 2963
[54] Vinet P, Ferrante J, Rose J H and Smith J R 1987 *J. Geophys. Res.* **92** 9319
[55] Vinet P, Rose J H, Ferrante J and Smith J R 1989 *J. Phys.: Condens. Matter* **1** 1941
[56] Gaurav S, Sharma B S, Sharma S B and Upadhyaya S C 2002 *Physica* B **322** 328
[57] Rose J H, Ferrante J and Smith J R 1981 *Phys. Rev. Lett.* **47** 675
[58] Rose J H, Smith J R and Ferrante J 1983 *Phys. Rev. Lett.* **28** 1835
[59] Smith J R, Rose J H, Ferrante J and Guinea F 1984 *Many-Body Phenomena at Surfaces* ed D Lengreth and H Sahl (New York: Academic)
[60] Jeanloz R 1989 *J. Geophys. Res.* **94** 5873
[61] Dodson B W 1987 *Phys. Rev.* B **35** 2619
[62] Davydov B I 1956 *Izv. Akad. Nauk SSSR, Ser. Geofiz.* **12** 1411
[63] Zharkov V N and Kalinin V A 1971 *Equations of State for Solids at High Pressures and Temperatures* (New York: Consultants Bureau) p 257 (Translated from Russian)
[64] Pack D C, Evans W M and James H J 1948 *Proc. Phys. Soc.* **60** 1
[65] Davis L A and Gordon R B 1967 *J. Chem. Phys.* **46** 2650
[66] Grover R, Getting C and Kennedy G C 1973 *Phys. Rev.* B **7** 567
[67] Raju S, Sivasubramanian K and Mohandas E 2002 *Physica* B **324** 312
[68] Stacey F D 2000 *Geophys. J. Int.* **143** 621
[69] Meenakshi S and Sharma B S 1999 *High Temp.—High Pressures* **31** 259
[70] Tallon J L 1980 *J. Phys. Chem. Solids* **41** 837
[71] Hemley R J, Mao H K, Finger L W, Jephcoat A P, Hazen R M and Zha C S 1990 *Phys. Rev.* B **42** 6458
[72] Vashchenko V Y and Zubarev V N 1963 *Sov. Phys.—Solid State* **5** 653
[73] Brennan B J and Stacey F D 1979 *J. Geophys. Res.* **84** 5535
[74] Moruzzi V L, Janak J F and Williams A R 1978 *Calculated Electronic Properties of Metals* (New York: Pergamon)
[75] Elsasser W M 1951 *Science* **113** 105
[76] Holzapfel W B 1990 *Molecular Solids under Pressure* ed R Pucci and G Piccitto (Amsterdam: North-Holland) p 61
[77] Holzapfel W B 1991 *Europhys. Lett.* **16** 67
[78] Thomas L H 1927 *Proc. Camb. Phil. Soc.* **23** 542
[79] Fermi E 1928 *Z. Phys.* **48** 73
[80] Stacey F D 2005 *Rep. Prog. Phys.* **68** 341
[81] Parsafar G and Mason E A 1994 *Phys. Rev.* B **49** 3049
[82] Shanker J, Kushwah S S and Kumar P 1997 *Physica* B **239** 337
[83] Poirier J P and Tarantola A 1998 *Phys. Earth Planet. Inter.* **109** 1
[84] Deng X Q and Yan Z T 2002 *High Temp.–High Pressures* **34** 387
[85] Kunc K, Loa I and Syassen K 2003 *Phys. Rev.* B **68** 094107
[86] Carter W J, Marsh S P, Fritz J N and McQueen R G 1971 *Accurate Characterization of the High Pressure Environment* Special Publication, No 326 ed E C Lyod (Washington, DC: NBS) p 147
[87] Fritz J N, Marsh S P, Carter W J and McQueen R G 1971 *Accurate Characterization of the High Pressure Environment* Special Publication, No 326 ed E C Lyod (Washington, DC: NBS) p 201
[88] Hixson R S and Fritz J N 1992 *J. Appl. Phys.* **71** 1721
[89] Nellis W J, Moriarty J A, Mitchell A C, Ross M, Dandrea R G, Aschcroft N W, Holmes N C and Gathers G R 1988 *Phys. Rev. Lett.* **60** 1414
[90] Simmons G and Wang H 1971 *Single Crystal Elastic Constants and Calculated Aggregate Properties* 2nd edn (Cambridge: MIT)
[91] Kittel C 1976 *Introduction to Solid State Physics* 5th edn (New York: Wiley)

[92] Ullmann W and Pan'kov V L 1976 *Veroff Zentralinstitut fur Phys. der Erde, Potsdam* **41** 1
[93] Greene R G, Luo H and Ruoff A L 1994 *Phys. Rev. Lett.* **73** 2075
[94] Swenson C A 1968 *J. Phys. Chem. Solids* **29** 1337
[95] Vant't Klooster P, Traphenters N J and Biswas S N 1979 *Physica* B **97** 65
[96] Anderson O L 1966 *J. Phys. Chem. Solids* **27** 547
[97] Holzapfel W B 1997 *High-Pressure Techniques in Chemistry and Physics* ed W B Holzapfel and N S Isaacs (New York: Oxford University Press) p 47
[98] Wang K and Reeber R R 1997 *High Temp. Mater. Sci.* **36** 185
[99] Mao H K and Bell P M 1979 *J. Geophys. Res.* **84** 4533
[100] Anderson O L and Andreatch P Jr 1966 *J. Am. Ceram. Soc.* **49** 404
[101] Spetzler H, Sammis C G and O' Connell R J 1972 *J. Phys. Chem. Solids* **33** 1727
[102] Kim H S, Graham E K and Voigt D E 1989 *Trans. Am. Geophys. Union* **70** 1368
[103] Oganov A R and Dorogokupets P I 2003 *Phys. Rev.* B **67** 224110
[104] Schlosser H and Ferrante J 1988 *Phys. Rev.* B **37** 4351
[105] Cohen R E, Gulseren O and Hemley R J 2000 *Am. Mineral.* **85** 338
[106] Hama J and Suito K 1996 *J. Phys.: Condens. Matter* **8** 67
[107] Jeanloz R 1988 *Phys. Rev.* B **38** 805
[108] Holzapfel W B 1996 *Rep. Prog. Phys.* **59** 29
[109] Barnes J F 1967 *Phys. Rev.* **153** 269
[110] Macdonald R A and Shukla R C 1985 *Phys. Rev.* B **32** 4961
[111] Boogerd P, Verbeek H J, Stuivinga M and van der Steen A C 1995 *J. Appl. Phys.* **78** 5335
[112] Chiang K-N, Chou C-Y, Wu C-J and Yuan C-A 2006 *Appl. Phys. Lett.* **88** 171904
[113] Kazanc S, Ciftci Y O, Colakoglu K and Ozgen S 2006 *Physica* B **381** 96
[114] Barton M A and Stacey F D 1989 *Phys. Earth Planet Inter.* **56** 311
[115] Stacey F D 1998 *Phys. Earth Planet Inter.* **106** 219
[116] Anderson M S and Swenson C A 1983 *Phys. Rev.* B **28** 5395
[117] Keane A 1954 *Aust. J. Phys.* **7** 322
[118] Truesdell C 1966 *The Mechanical Foundations of Elasticity and Fluid Dynamics* (New York: Gordon and Breach)
[119] Perrin G and Delannoy M 1977 *J. Mech. Phys. Solids* **25** 41
[120] Ruoff A L and Chhabildas L C 1978 *6th AIRAPT Conf.: High Pressure-Science and Technology* vol 1, ed K D Timmerhaus and M S Barber (New York: Plenum) pp 19–32
[121] Hofmeister A M 1993 *Geophys. Res. Lett.* **20** 635
[122] Zhang Y, Zhao D, Matsui M and Guo G 2006 *Phys. Chem. Miner.* **33** 126
[123] Solozhenko V L, Kurakevych O O, Solozhenko E G, Chen J and Parise J B 2006 *Solid State Commun.* **137** 268
[124] Holl C M, Smyth J R, Munghani M H, Amulele G M, Sekar M, Frost D J, Prakapenka V B and Shen G 2006 *Phys. Chem. Minerals* **33** 192